

Lattice relaxation of DX -like donors in $Zn_xCd_{1-x}Te$

K. Khachatryan, M. Kaminska, and E. R. Weber

Department of Materials Science and Mineral Engineering, University of California, Berkeley, California 94720

P. Becla

Francis Bitter National Magnet Laboratory, Massachusetts Institute of Technology, Cambridge, Massachusetts 02139

R. A. Street

Xerox Corporation, Palo Alto Research Center, 3333 Coyote Hill Road, Palo Alto, California 94304

(Received 10 June 1988; revised manuscript received 22 August 1989)

The configuration-coordinate diagram was constructed for deep relaxed In impurities in $Zn_xCd_{1-x}Te$. On the basis of the Hall effect, deep-level transient spectroscopy, photoionization, and photoluminescence measurements it was shown that In donors in $Zn_xCd_{1-x}Te$ possess analogous properties to the so-called DX center in $Al_xGa_{1-x}As$. The absence of paramagnetic resonance from In donors suggests that In atoms form a mixture of In^+ and In^{3+} ions, in equal numbers. A persistent photo-EPR signal from mobile photoelectrons was observed after illumination at $g = 1.316$ and could be thermally annealed. A strong broad, donor-acceptor-pair luminescence was found, with periodically spaced phonon lines at high excitation powers.

INTRODUCTION

Donors in $Zn_xCd_{1-x}Te$ ternary II-VI compounds exhibit low-temperature, persistent photoconductivity, if the Zn mole fraction is large enough.¹ This behavior is similar to that of a DX center² in $Al_xGa_{1-x}As$. The role of Zn in $Zn_xCd_{1-x}Te$ corresponds to that of Al in $Al_xGa_{1-x}As$, i.e., addition of Zn to CdTe converts a shallow hydrogenic donor in CdTe into a deep donor. Lang and Logan³ and Toyozawa⁴ explained persistent photoconductivity in n -type $Zn_xCd_{1-x}Te$ by large lattice relaxation, similar to the case of the DX center. Persistent photoconductivity was also observed in CdTe:Cl (the effect increases under pressure).⁵ In this paper, for the first time we shall investigate In deep donor in $Zn_{0.2}Cd_{0.8}Te$ with a combination of EPR, deep-level transient spectroscopy (DLTS), resistivity measurements, and photoluminescence, and show that the observed data can be as well explained by the lattice relaxation model. The conversion of the shallow hydrogenic donor into a deep relaxed one can be achieved not only by Zn addition, but also by applying hydrostatic pressure.⁶ This is also similar to the case of the DX center, which also can be produced if hydrostatic pressure is applied to n -type GaAs.⁷ For the case of DX centers, the possibility of converting a shallow isolated substitutional donor in GaAs into the DX center by the hydrostatic pressure constituted proof that the DX center is an isolated substitutional donor. Similarly, the possibility of converting a shallow substitutional donor in CdTe into a deep relaxed donor by the hydrostatic pressure⁶ constitutes strong evidence that the deep relaxed donors in CdTe under pressure and $Zn_xCd_{1-x}Te$ are isolated substitutional donors.

The study of the ternary II-VI $Zn_xCd_{1-x}Te$ system also has two major advantages over the $Al_xGa_{1-x}As$ sys-

tem. First, bulk crystals of $Zn_xCd_{1-x}Te$ can be grown by the Bridgman method, whereas $Al_xGa_{1-x}As$ can only be grown as a thin epitaxial layer. This makes $Zn_xCd_{1-x}Te$ particularly valuable for electron paramagnetic measurements of relaxed donors, exhibiting persistent photoconductivity. The second advantage is the possibility of introducing shallow hydrogenic donors by Al or I doping (Cl, Br, In, and Ga form deep relaxed donors).⁶ This is in contrast to $Al_xGa_{1-x}As$ where all donors form the deep DX centers if the Al concentration is high enough.

Toyozawa⁸ proposed the metastable behavior of the DX center to be caused by extrinsic self-trapping⁸⁻¹⁰ similar to that in a polaron. In the case of a polaron only the lattice distortion itself is sufficient to create a self-trapped state. In the case of the DX center, lattice distortion alone is not sufficient (otherwise polarons would have been observed in undoped $Al_xGa_{1-x}As$), but needs to be assisted by the short-range donor impurity potential. The short-range donor impurity potential depends on the chemical properties of the donor impurity. For the case of an isolated donor atom the greater the difference in electronegativity of the donor atom and the host lattice atom it substitutes, the greater the short-range impurity potential. Application of extrinsic self-trapping theory to $Zn_xCd_{1-x}Te$ allows us to understand why Al and I form shallow hydrogenic donors in $Zn_xCd_{1-x}Te$, whereas In, Ga, Br, and Cl form deep relaxed donors. Indeed, Al is the most metallic and the least electronegative element of the Cd-site group-III donors. Therefore the short-range impurity potential of Al is the smallest and its sum with the lattice relaxation energy is not enough to lead to electron localization. Similarly, I is the least electronegative element of the Te-site group-VII donors and therefore it does not form a deep relaxed DX -like donor.

EXPERIMENT

In this paper, we have investigated In-doped $\text{Zn}_{0.2}\text{Cd}_{0.8}\text{Te}$. The room-temperature electron concentration was $6 \times 10^{16} \text{ cm}^{-3}$. Cl-doped samples of $\text{Zn}_{0.2}\text{Cd}_{0.8}\text{Te}$, with the room-temperature electron concentration due to Cl donors of 3.4×10^{14} , were also used. The crystals were grown from the melt at the speed of about 1.4 mm/h. The Cl doping was achieved by adding ZnCl_2 and In doping by adding In metal into the melt. The temperature gradient in the furnace was $50^\circ\text{C}/\text{cm}$. The material in the quartz ampule was covered by graphite, and the ampule was then put into the Bridgman furnace. The dopant was introduced directly into the melt. After growth the crystal was cut into slices and the slices were then annealed in cadmium vapors at 0.02 atm at 600°C for 5 d. The purpose of annealing was to decrease the concentration of intrinsic acceptors, presumably Cd vacancies, to the acceptable level of the order of $10^{15}/\text{cm}^3$. This characteristic value of residual intrinsic acceptor concentration was determined by the Hall measurements on undoped *p*-type samples.

A Bruker EPR ER-200D spectrometer, working in the X band (around 9.4 GHz) and up to 100 kHz modulation amplitude, was used for these studies. Temperature variation was obtained with a He gas-flow cryostat allowing the stabilization of sample temperatures between 8 and 300 K with 0.2 K precision. The EPR cavity had an optical window so that the sample could be illuminated *in situ*. The photoluminescence studies were done at Xerox PARC. An argon laser was used for photoexcitation and a germanium detector was used for detection of photoluminescence. A standard DLTS setup with the boxcar connected to the *x-y* plotter was used. In the photoionization cross-section measurement the rate of conductivity change $d\sigma/dt$ was measured for different wavelengths at liquid-helium temperature. A Zeiss monochromator and an Oriol lamp were used for illumination with monochromatic light. An EPR cryostat was used for cooling the sample. The sample, connected to the wires, was put into the quartz tube sealed from one end. The quartz tube was then put into the EPR cavity, and cooled down by liquid-helium flow. After each measurement, the persistent photoconductivity was annealed by heating up the sample to about 100 K and cooling it back to liquid-helium temperature before subsequent measurements are made. For the temperature-dependent Hall-effect measurement, a computer-controlled automatic system was used. The sample was slowly cooled down by liquid-helium flow.

**ABSENCE OF THE EPR SIGNAL
AND POSSIBILITY OF NEGATIVE *U*
OF DEEP INDIUM DONOR IN $\text{Zn}_{0.2}\text{Cd}_{0.8}\text{Te}$**

The electron-paramagnetic-resonance experiment was made on an In-doped $10 \times 3 \times 3 \text{ mm}^3$ piece of $\text{Zn}_{0.2}\text{Cd}_{0.8}\text{Te}$ with a room-temperature electron concentration of $6 \times 10^{16} \text{ cm}^{-3}$. Although the amount of indium atoms was 4 orders of magnitude greater than the sensitivity limit of the EPR spectrometer, no EPR signal was

detected after cooling down in the dark.

The EPR measurements on a $10 \times 3 \times 3 \text{ mm}^3$ piece of $\text{Zn}_{0.2}\text{Cd}_{0.8}\text{Te}:\text{In}$ after illumination were impossible because the persistent photoconductivity resulted in such a low *Q* factor of the cavity that no EPR measurements could be performed. To make the measurements after illumination, a thin needle-shaped sample had to be used. We took a needle-shaped sample of 1 mm diameter, and 4 mm length. After photoionization, the persistent EPR signal with $g=1.316$ and a width of 68 G [Fig. 1(a)] from In-doped $\text{Zn}_{0.2}\text{Cd}_{0.8}\text{Te}$ was observed. It disappeared only when the sample was heated up to the annealing temperature of about 90 K and subsequently cooled to the initial temperature of 20 K. The EPR signal with the same *g* value was obtained from the samples doped predominantly with Al (which is a shallow donor) before illumination. Absence of the hyperfine structure of the signal and disappearance of the signal when persistent photoconduc-

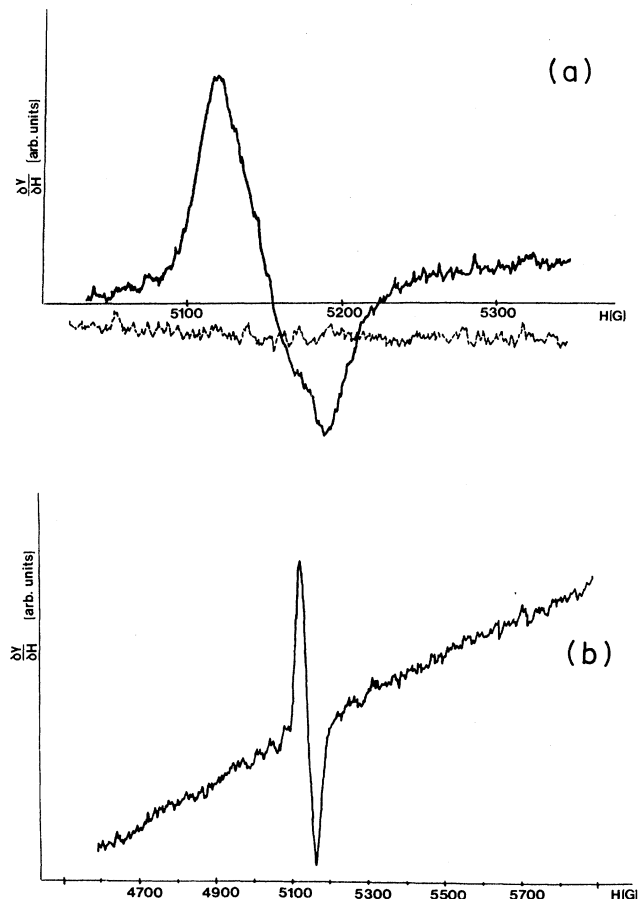


FIG. 1. (a) Light-induced persistent EPR signal from In-doped $\text{Zn}_{0.2}\text{Cd}_{0.8}\text{Te}$ (solid line) measured at $T=20 \text{ K}$ at $\omega=0.490 \text{ GHz}$. The signal disappears (dashed line) when the sample is heated up to 90 K and then is cooled down again to the initial temperature of 20 K. (b) The same signal on the background of the positive slope of the baseline due to negative magnetoresistance.

tivity is annealed indicate that the signal must be due to mobile photoelectron paramagnetic resonance. The width of the persistent photo-EPR (PEPR) signal increased with the increase in concentration of photoelectrons (increase in illumination dose). The persistent PEPR signal with the same g value was also observed from the Cl-doped $\text{Zn}_{0.2}\text{Cd}_{0.8}\text{Te}$. The width of the PEPR signal from the Cl-doped sample was 45 G, which is less than 68 G for the case of an In-doped sample because the photoelectron concentration is much less for the case of the Cl-doped sample.

A possible explanation of that is that the ground state of In in $\text{Zn}_{0.2}\text{Cd}_{0.8}\text{Te}$ is diamagnetic, i.e., it has a singlet electron pair rather than one electron on it. An alternative explanation by extremely broad EPR lines, which could not be observed, or a line with $g < \frac{1}{2}$ that requires magnetic fields outside the range of the magnet is also possible. Since the total number of donor electrons is equal to the number of donor atoms, electron pairing results in the disproportionation reaction



Such a disproportionation reaction is described by the negative Hubbard energy U .

The disproportionation reaction is well known in inorganic chemistry, especially for heavy group-III A elements, such as Ga, In, and Tl. An example of such a disproportionation is group-III A chalcogenides, such as InTe, TlSe, or TlTe,¹¹ where the In (or Tl) atom is apparently divalent, but in reality is a mixture of In^{+} and In^{3+} ions in different crystallographic environments. For example, in TlSe, Tl^{3+} and Se ions form $(\text{TlSe}_2)^{-n}$ chains, whereas Tl^{+} ions are situated in between the different chains.¹¹

However, in the case of the DX centers in $\text{Al}_x\text{Ga}_{1-x}\text{As}$, very recent magnetic susceptibility measurements¹² indicated that the DX center is a paramagnetic, positive U center even though no EPR signal from the ground state could be observed.

Another interesting phenomenon is the negative magnetoresistance of both In- or Cl-doped $\text{Zn}_{0.2}\text{Cd}_{0.8}\text{Te}$ samples after photoionization at low temperatures (from 4.2 K to the persistent photoconductivity annealing temperature). The negative magnetoresistance manifests itself in the positive slope of the EPR baseline [Fig. 1(b)]. The resistivity of the sample in the magnetic field is

$$\rho = \rho_0 + \beta H^2 , \quad (2)$$

where β is the coefficient for magnetoresistance of the sample, ρ_0 is the resistivity of the sample in the absence of magnetic field, and H is the magnetic field. Since the EPR spectrometer output is the derivative of the microwave absorption by the magnetic field, and the microwave absorption is inversely proportional to the resistivity of the sample, the shift of the EPR baseline would therefore be equal to

$$\Delta = -2A\beta H / \rho^2 \quad (3a)$$

and the slope of the EPR baseline would then give the value of the coefficient for magnetoresistance β ,

$$S = \partial\Delta / \partial H = -2A\beta / \rho^2 , \quad (3b)$$

where

$$A = \int E^2(\mathbf{r}) d^3r \quad (4)$$

is a constant depending on the position of the sample in the microwave cavity and the distribution of the electric component of the microwave field $\mathbf{E}(\mathbf{r})$ in the cavity.

CONFIGURATION-COORDINATE DIAGRAM OF INDIUM DONOR IN $\text{Zn}_x\text{Cd}_{1-x}\text{Te}$

In-doped $\text{Zn}_{0.2}\text{Cd}_{0.8}\text{Te}$ exhibited low-temperature persistent photoconductivity which annealed out around 80–90 K. The photoionization threshold of a deep donor in $\text{Zn}_{0.2}\text{Cd}_{0.8}\text{Te}$ was measured to be 0.7 eV. The photoionization curve was about 0.2 eV broad (Fig. 2), with the photoionization cross section exponentially increasing in the photon-energy region 0.7–0.9 eV. Though some widening can be accounted for by a possible alloy broadening effect, the width of 0.2 eV suggests strong defect coupling with phonons.

The slope of the $\ln n$ versus $1000/T$ corresponds to the Fermi energy position of 0.067 eV (Fig. 3). The difference between thermal and optical depths indicates a large Stokes shift, similar to that of the DX center. The emission barrier, measured by DLTS, was 0.29 eV (Fig. 4). Direct capture-rate measurements by the DLTS technique revealed logarithmic capture behavior [capacitance is proportional to the logarithm of the filling pulse duration (Fig. 5)]. Though logarithmic capture can be expected for trapping by charged dislocations, it was also reported for DX centers in $\text{Al}_x\text{Ga}_{1-x}\text{As}$.¹³ Caswell *et al.*¹⁴ explained the logarithmic capture by DX centers by charge of the capture barrier when the quasi-Fermi level shifts upon capture. The very large magnitude of the

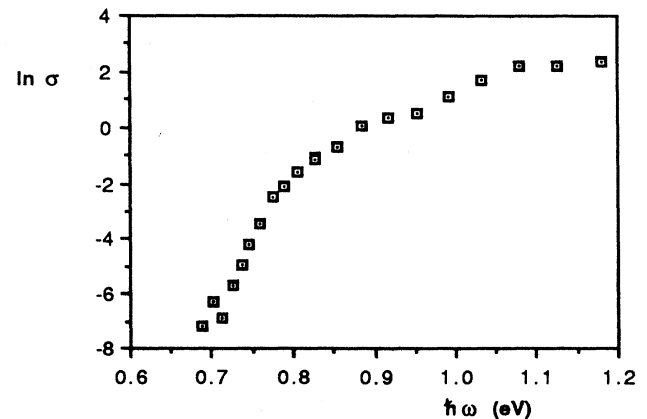


FIG. 2. Photoionization curve of In-doped $\text{Zn}_{0.2}\text{Cd}_{0.8}\text{Te}$ at 10 K. Logarithm of the photoionization cross section in arbitrary units is plotted vs the energy of light.

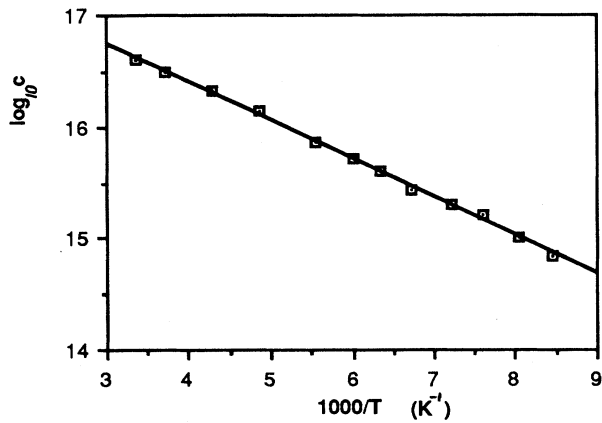


FIG. 3. Logarithm of electron concentration per cm^3 in In-doped $\text{Zn}_{0.2}\text{Cd}_{0.8}\text{Te}$ measured by Hall effect vs inverse lattice temperature.

DLTS signal from In in $\text{Zn}_{0.2}\text{Cd}_{0.8}\text{Te}$ $dC/C \approx \frac{1}{3}$ indicates that it was coming from the main electrically active impurity, i.e., the In donor. The logarithmic capture makes it very difficult to extract the capture-behavior value from the DLTS measurements. Measurement of the capture barrier was made by studying the temperature dependence of the rate of resistivity recovery after the illumination is turned off in the temperature range 77–90 K. The beginning of the resistivity recovery is shown in Fig. 6. The speed of the resistance increase, dR/dt , is proportional to the capture cross section. In the first moment after the illumination is turned off, there is a jump in sample resistance; but after that the resistance increased *linearly* with time, at liquid-nitrogen temperature for many hours. This can be explained if the electron-capture rate is proportional to the *square* of the uncap-tured electron concentration

$$dn/dt \sim -vn^2\sigma, \quad (5)$$

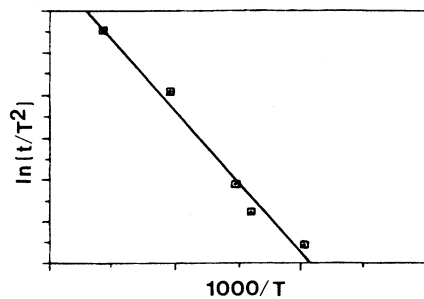


FIG. 4. Arrhenius plot of logarithm of emission time constant (in μs) divided by temperature squared vs inverse temperature measured on In-doped $\text{Zn}_{0.2}\text{Cd}_{0.8}\text{Te}$. The emission barrier determined from the plot is 290 meV.

where v is thermal velocity of electrons, n is free-electron concentration, and σ is the capture cross section. The quadratic capture should be expected for a negative- U donor or for a positive- U donor in the absence of shallow donors. Dividing (6) by n^2 , one obtains

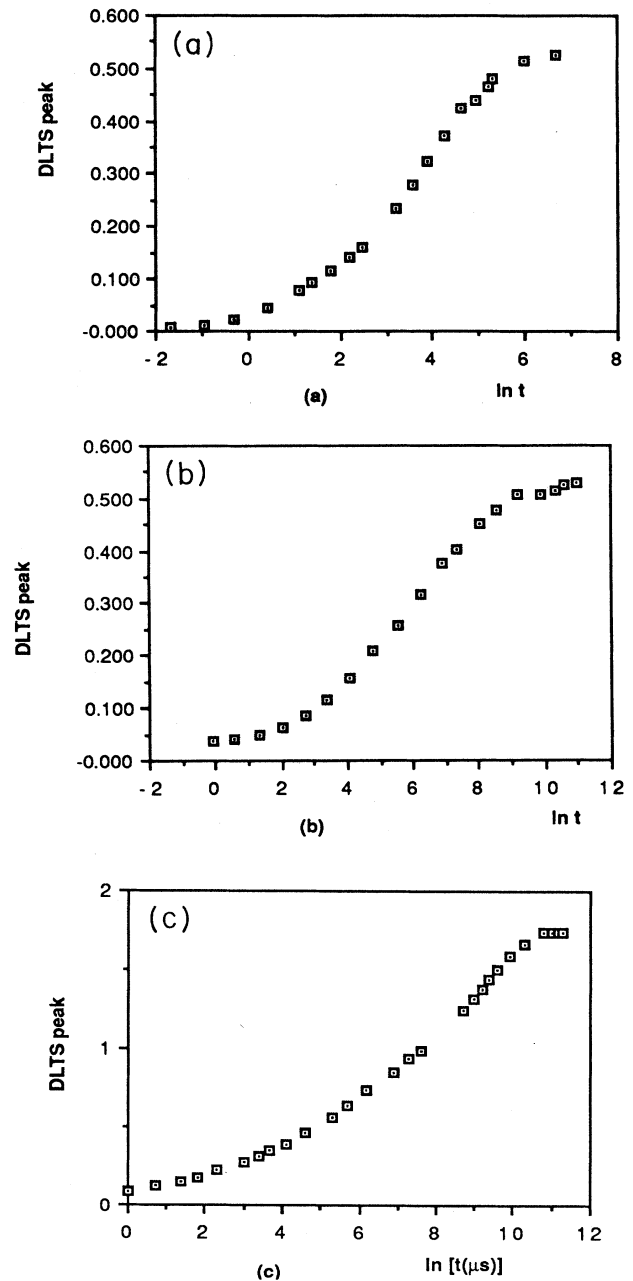


FIG. 5. The DLTS transient (arbitrary units) as a function of filling pulse duration (in μs) from $\text{Zn}_{0.2}\text{Cd}_{0.8}\text{Te}$ doped by (a) shallow Al and deep relaxed Ga donors at 187 K, (b) shallow Al and deep relaxed Ga donors at 147 K, and (c) a deep indium donor at 121.5 K.

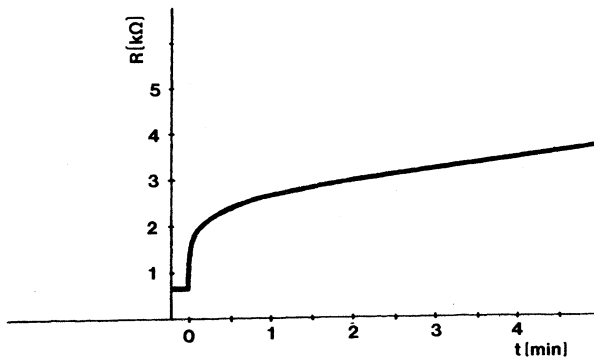


FIG. 6. Resistance transient of the sample of In-doped $\text{Zn}_{0.2}\text{Cd}_{0.8}\text{Te}$ at liquid-nitrogen temperature after illumination is switched off. An initial small positive jump in resistance is followed by a slow (lasting for many hours) linear increase in resistance with time.

$$d(1/n)/dt \sim v \quad (6)$$

or, since $R \sim 1/en\mu$,

$$dR/dt \sim v/\mu. \quad (7)$$

The electron mobility after photoionization in the temperature range 70–90 K is determined mostly by a Coulombic charge scattering by ionized positively charged donors, proportional to $T^{3/2}$. Thermal electron velocity is proportional to \sqrt{T} (T is temperature). Using that in (7) one can extract the capture-activation barrier from the slope of a plot of $\ln [T(dR/dt)]$ versus $1000/T$ (Fig. 7),

$$E_c = -k_B d \ln [T(dR/dt)] / d(1/T). \quad (8)$$

For the case of In in $\text{Zn}_{0.2}\text{Cd}_{0.8}\text{Te}$, $E_c = 0.13$ eV. To ob-

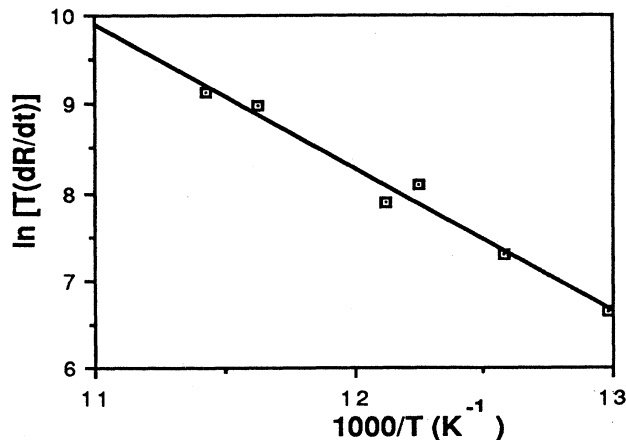


FIG. 7. Plot of $\ln [T(dR/dt)]$ vs $1000/T$. T is the temperature in K and dR/dt is the speed of resistance increase in $\text{k}\Omega/\text{s}$.

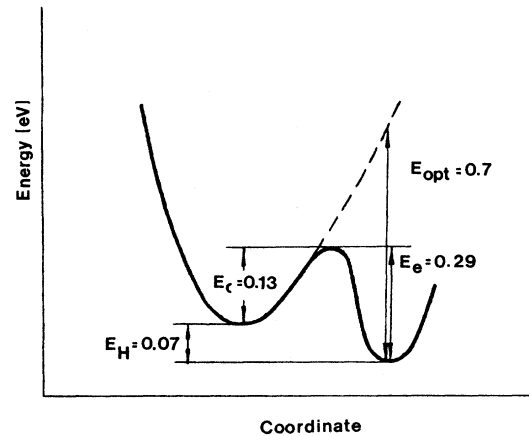


FIG. 8. Configuration-coordinate diagram of the indium donor in $\text{Zn}_{0.2}\text{Cd}_{0.8}\text{Te}$. E_{opt} , E_H , E_c , and E_e are optical and thermal depths of the level and capture and emission barriers.

tain agreement between the thermal depth of the donor with the difference between the emission barrier 0.29 eV and the capture barrier 0.14 eV, one has to assume that the thermal depth of the In donor in $\text{Zn}_{0.2}\text{Cd}_{0.8}\text{Te}$ is twice the slope of a plot of $\ln n$ versus $1000/T$ (Fig. 8). This can be the case in the positive- U model for uncompensated material ($n \gg N_A$) or in the negative- U case. In the negative- U case the factor of 2 is due to two electrons localized on the donor, the Fermi energy always being stabilized in between $+0$ and $0/-$ levels, regardless of the acceptor concentration.

Cl-doped $\text{Zn}_{0.2}\text{Cd}_{0.8}\text{Te}$ was also found to exhibit persistent photoconductivity, confirming the results of Ref. 1. In this case, the very small, 3.4×10^{14} , room-temperature electron concentration made temperature-dependent Hall and DLTS measurements very difficult. To determine the persistent photoconductivity annealing temperature, a different, contactless method was used. The conductivity of the sample was monitored by the Q factor of the microwave cavity of the EPR spectrometer. The Q factor could be visually seen on the oscilloscope screen in the tune mode, when the microwave absorption of the loaded cavity was scanned as a function of the microwave frequency. The sample was illuminated *in situ* in the EPR cavity with optical access at liquid-helium temperature. After that, the temperature was raised and the temperature when the Q factor started to increase was noted as the photoconductivity annealing temperature. In this way, the photoconductivity annealing temperature of Cl-doped $\text{Zn}_{0.2}\text{Cd}_{0.8}\text{Te}$ was measured to be around 150 K.

DONOR-ACCEPTOR PAIR LUMINESCENCE

The photoluminescence from $\text{Zn}_{0.2}\text{Cd}_{0.8}\text{Te}:\text{In}$ or Cl (Fig. 9) consisted of two peaks—a sharp higher-energy peak and a broad low-energy band. The sharp higher-energy peak could hardly be distinguished at low temperatures. However, at higher temperatures it becomes

dominant. Excitation power dependence of the intensity of these peaks showed no saturation of the high-energy sharp peak, whereas the lower-energy broad peak saturated with increasing argon-laser power. The photoluminescence from mixed Al- and Ga-doped samples, on the other hand, showed only the broad lower-energy peak. The half-width of the broad band in the In-doped sample was

0.13 in Al- and Ga-doped material, 0.07 eV for 2 mW excitation power, and 0.11 eV in the Cl-doped sample.

The shape of the broad band changed with excitation power; the maximum shifted and the width sometimes increased or sometimes decreased with an increase in excitation power. A change in line shape with excitation power is a characteristic feature of the donor-acceptor-pair (DAP) luminescence.¹⁵ The broad band from Al- and Ga-doped material was in the energy range from 1.38 to 1.59 eV, and shifted to lower energies compared to the other two In- and Cl-doped samples. The height of the broad band was of the same order of magnitude in all the three samples, although, judging from the Hall data, the donor concentration in the Cl-doped sample was 2 orders of magnitude less than in the In-doped sample. On the other hand, undoped *p*-type (due to intrinsic acceptors) $\text{Zn}_x\text{Cd}_{1-x}\text{Te}$, as shown by Triboulet *et al.*,¹⁶ does not show the broad lower-energy emission band. This indicates that donor doping is required to create the broad photoluminescence band, and yet the intensity of the photoluminescence is limited by the concentration of another defect, a coactivator. This picture is consistent with donor-acceptor-pair luminescence. Though no acceptors were deliberately introduced during the crystal growth, intrinsic acceptors, presumably Cd vacancies, are always present after crystal growth and even after thermal annealing in Cd vapor (in concentration about $10^{15}/\text{cm}^3$), designed to decrease the concentration of intrinsic acceptors. In heavily donor-doped $\text{Zn}_x\text{Cd}_{1-x}\text{Te}$ samples, it is therefore this intrinsic acceptor concentration that determines the intensity of the broad band. More evidence of the donor-acceptor-pair nature of the broad energy band is the observed change in the shape of the broad band with excitation power (Fig. 10). The sharp high-energy peak, on the other hand, does not saturate and at high excitation powers (~ 100 mW) becomes dominant. This indicates that the sharp peak is due to the bound exciton.

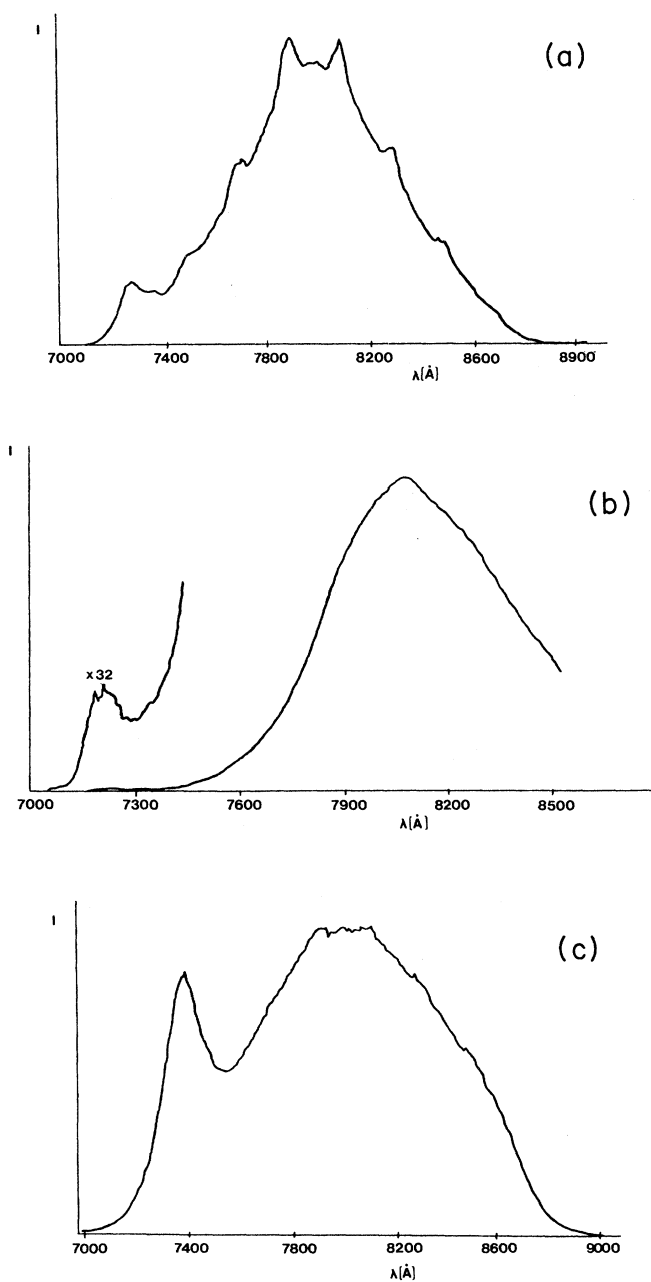


FIG. 9. Photoluminescence from indium donor in $\text{Zn}_{0.2}\text{Cd}_{0.8}\text{Te}$ in arbitrary units. (a) At 2 K, laser power 23 mW. (b) At 2 K, laser power 0.8 mW. The bound-exciton peak is enlarged 32 times. (c) At 150 K, laser power 23 mW. The scale in (b) and (c) is $\frac{2}{9}$ and $\frac{1}{18}$ of the scale in (a), respectively.

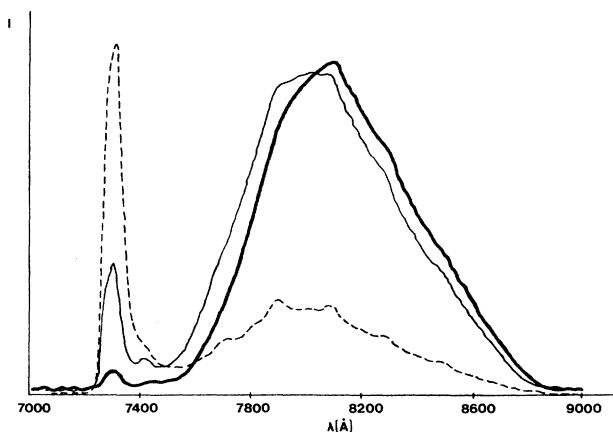


FIG. 10. Photoluminescence from $\text{Zn}_{0.2}\text{Cd}_{0.8}\text{Te}:\text{Cl}$ at 2 K in arbitrary units. The thick solid line, thin solid line, and dashed line correspond to 2, 9, and 100 mW excitation powers, respectively.

The lower-energy broad band, at high laser power, exhibits fine phonon structure. The phonon peaks are equidistant, spaced by 38 meV for the case of In-doped material. The spacing of 38 meV is characteristic of coupling with optical phonons.

Both large width and fine phonon structure are characteristic of donor-acceptor-pair luminescence in a wide variety of III-V and II-VI compounds, such as, for example, GaP or ZnS (Ref. 17) or $\text{Al}_x\text{Ga}_{1-x}\text{As}:\text{Si}$.^{18,19} It occurs regardless of presence or absence of a low-temperature persistent photoconductivity. In any case, since the sample is being illuminated by the laser light during a photoluminescence experiment, it is the *metastable hydrogenic state* and not the deep relaxed ground state of a deep In or Cl donor that gives rise to the observed donor-acceptor-pair luminescence. The periodic phonon structure could be due to the coupling of a deep intrinsic acceptor to the lattice.

SUMMARY

Measured values of the thermal depth, emission, capture, and optical ionization barriers indicate that Lang's

configuration-coordinate diagram model can be used to describe the properties of In donor in $\text{Zn}_{0.2}\text{Cd}_{0.8}\text{Te}$. Together with the effect of Zn mole fraction on the depth of the relaxed In donor, this indicates the similarity between properties of the In donor in $\text{Zn}_{0.2}\text{Cd}_{0.8}\text{Te}$ and the *DX* center in $\text{Al}_x\text{Ga}_{1-x}\text{As}$. A large PEPR signal from mobile photoelectrons after illumination from a small needlelike piece of $\text{Zn}_{0.2}\text{Cd}_{0.8}\text{Te}$ and the absence of an EPR signal from In donors in the dark were observed. Broad donor-acceptor-pair luminescence from the *n*-type $\text{Zn}_{0.2}\text{Cd}_{0.8}\text{Te}$ with fine phonon structure was found.

ACKNOWLEDGMENTS

We thank D. Bliss for his help in using the computer-controlled temperature-dependent Hall apparatus. We thank W. Sham for his help in using his DLTS setup. We thank Professor P. Yu and Professor E. E. Haller for the use of their equipment and valuable discussions. We thank Professor L. Brewer for stimulating discussions. This work was supported in part by the Director, Office of Energy Research, Office of Basic Energy Sciences, Materials Science Division, of the U.S. Department of Energy under Contract No. DE-AC03-76SF00098.

¹B. C. Burkey, R. P. Khosla, J. R. Fischer, and D. L. Losee, *J. Appl. Phys.* **47**, 1095 (1976).

²D. V. Lang and R. A. Logan, *Phys. Rev. Lett.* **39**, 635 (1977).

³D. V. Lang, in *Deep Centers in Semiconductors*, edited by S. T. Pantelides (Gordon and Breach, New York, 1987).

⁴Y. Toyozawa, *Physica B+C* **116B**, 7 (1983).

⁵R. Legros, Y. Marfaing, and R. Triboulet, *J. Phys. Chem. Solids* **39**, 179 (1978).

⁶G. W. Iseler, J. A. Kafalas, J. J. Strauss, H. F. McMillan, and R. H. Bube, *Solid State Commun.* **10**, 619 (1972).

⁷M. Mizuta, M. Tachikawa, H. Kukimoto, and S. Minomura, *Jpn. J. Appl. Phys.* **24**, L143 (1985).

⁸Y. Toyozawa, *Solid State Electron.* **21**, 1313 (1978); in *Relaxation of Elementary Excitations*, edited by R. Kubo and E. Hanamura (Springer, New York, 1980), p. 3.

⁹Y. Toyozawa and Y. Shinozuka, *J. Phys. Soc. Jpn.* **48**, 472 (1980).

¹⁰D. Emin and T. Holstein, *Phys. Rev. Lett.* **36**, 323 (1976); D. Emin, M. Hillery, and N. L. H. Liu, *Phys. Rev. B* **35**, 641

(1987).

¹¹W. B. Pearson, *The Crystal Chemistry and Physics of Metals and Alloys* (Wiley-Interscience, New York, 1972).

¹²K. A. Khachaturyan, D. D. Awschalom, J. R. Rozen, and E. R. Weber (unpublished).

¹³T. N. Theis, T. F. Kuech, L. F. Palmateer, and P. M. Mooney, *IOP Conf. Proc. Ser. No. 74* (IOP, London, 1984), p. 241.

¹⁴N. S. Caswell, P. M. Mooney, S. L. Wright, and P. M. Solomon, *Appl. Phys. Lett.* **48**, 1093 (1986).

¹⁵P. J. Dean, *Prog. Cryst. Growth Charact.* **5**, 89 (1982).

¹⁶R. Triboulet, G. Neu, and B. Foutouhi, *J. Cryst. Growth* **65**, 262 (1983).

¹⁷P. J. Dean, in *Progress in Solid State Chemistry*, edited by J. O. McCaldin and G. Somorjai (Pergamon, New York, 1973), Vol. 8, p. 1.

¹⁸J. C. M. Henning and J. P. M. Ansems, *Semicond. Sci. Technol.* **2**, 1 (1987).

¹⁹J. C. M. Henning, J. P. M. Ansems, and A. G. M. de Nijs, *J. Phys. C* **17**, L915 (1984).